DOI: 10.2478/ata-2026-0007

Acta Technologica Agriculturae 1
Nitra, Slovaca Universitas Agriculturae Nitriae, 2026, pp. 51–60

USING NDWI FOR DIAGNOSING MOISTURE AVAILABILITY IN AGRICULTURAL AREAS SURVEYED WITH UAV

Asparuh I. ATANASOV

Technical University of Varna, Faculty of Mechanical Engineering, Department of Mechanics and Elements of Machines, Varna, Bulgaria

*correspondence: asparuh.atanasov@tu-varna.bg

The study investigates the feasibility of monitoring water content in the topsoil. The study was conducted over five growing seasons from 2019 to 2024. The primary instrument used was an unmanned aerial vehicle (UAV) equipped with a multispectral camera recording reflectance in the near-infrared (NIR) region. Data was collected by flying the UAV at an altitude of 100 m above agricultural areas to capture individual images. These images were then processed to create an orthomosaic, from which the WDVI index (Weighted Difference Vegetation Index) was generated. For comparison, the normalised difference vegetation index (NDVI), which assesses the crop's vegetation stage, was also used. The index values were compared with meteorological data collected from the specific field. The study showed a strong correlation before crop coverage reached 50% (R = 0.96 and R^2 = 0.94). With dense plant cover, the correlation was weaker (R = 0.87 and R^2 = 0.77).

Keywords: remote sensing; UAV; NDWI (Normalised Difference Water Index); precision agriculture; soil moisture

Several reflectance indices have been developed to assess soil moisture. One such index, the Water Stress Index (WSI), is an indicator of soil water content (Jensen et al., 1998). Based on this, the Weighted Difference Vegetation Index (WDVI) was developed, which tracks subtle changes in water content and effectively corrects for the reflectance of the soil background. The authors such as Yu et al. (2001) and Xu (2002) extracted water content information by analysing the reflectance characteristics of ground objects. An alternative is the NDWI (Normalised Difference Water Index), developed by McFeeters (1996). It yields positive values for water surfaces and negative (or zero) values for soil and vegetation (Alvaro et al., 2007).

Xu (2006) modified the NDWI for watershed mapping by replacing the *NIR* band with the shortwave infrared (SWIR) band. This Modified NDWI (MNDWI) improves water detection performance while effectively suppressing and even eliminating noise from soil and vegetation. Gao (1996) utilised frequency bands at 0.86 µm and 1.24 µm, which correspond to high reflectance from vegetation. Chandramohan et al. (2024) investigated the relationships between NDVI, NDWI, and Soil Moisture Index (SMI). Using Landsat satellite data, Afshari et al. (2025) compared NDVI, NDWI, and Land Surface Temperature (LST) in old-growth forests to analyse interactions trends between surface temperature and vegetation status. Alencar da Silva Allves (2024) and Atanasov et al. (2022) compared NDWI results to characterise spectral behaviour and determine which factors are most sensitive for identifying surface water. Wang et al. (2008) examined the potential for remote spectral assessment of topsoil moisture. Ustin et al. (1998) investigated the assessment of water content in shrubs as part of a fire risk assessment methodology. Due to the sowing depth of 3–5 cm for wheat, water content is key to the germination and early development of the crop (Toneva and Dimitrova, 2024; Koleva et al., 2025).

The aim of this study is to establish the applicability of the NDWI for remote monitoring of topsoil moisture using an UAV equipped with a multispectral camera. To achieve this, data from meteorological stations were collected and compared with the NDWI values generated from the multispectral camera imagery.

Material and methods

Study area

The study was conducted from 2019 to 2024 in agricultural fields within the Dobrich district, a part of the Dobruja region, Bulgaria. The observations sites are shown in Fig. 1. The fields are numbered 1 to 3, from left to right. Crop rotation was practised in all experimental fields, resulting in different planting locations for the crop varieties each year.

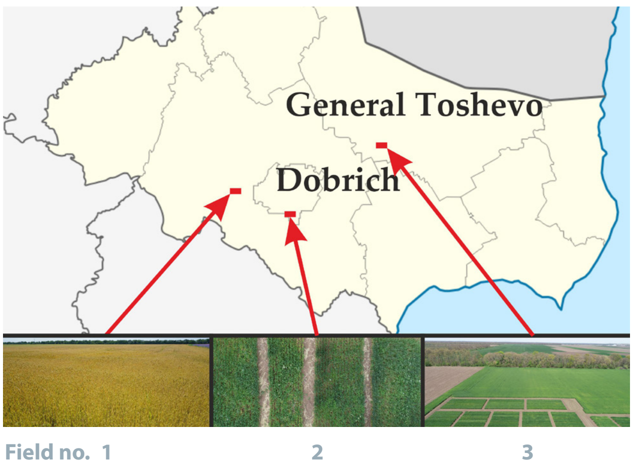

Fig. 1 The locations of the experimental fields

Field 1: An 18-hectare field located in the territory of Dobrich (coordinates: 43.548315, 27.756712).

Field 2: A 0.1-hectare experimental field at Dobruja Technological College in Dobrich (coordinates: 43.553346, 27.832154).

Field 3: A 24-hectare experimental field near the city of General Toshevo (coordinates: 43.656512, 28.018468).

UAV and camera system

Flight campaigns were conducted every ten days during the winter and every seven days during the active growing season for the studied crops from 2019 to 2024. The growing season for winter wheat extends from October to July of the following year. A total of 305 flights were conducted over the crops, capturing over 150,000 images. The data was processed using Pix4Dfields software (Pix4D, 2025).

The camera used for observation was a Mapir Survey3W RGN (Red, Green, Near-infrared) camera (Mapir, 2025). Flying at an altitude of 100 m with an image overlap of 80% (front and side), the resulting orthomosaic had an average resolution of 3.75 $cm \cdot px^{-1}$.

Flights were conducted at an altitude of 100 m above the terrain at a speed of 10 $m \cdot s^{-1}$. The camera was set to capture an image every second. The camera settings were fixed throughout the experiment: F-stop: 2.8; exposure time: 1/500 s; ISO speed: 100; focal length: 3 mm; digital zoom: 1.23x; EXIF version: 0220; colour representation: sRGB; bit depth: 24; vertical/horizontal resolution: 72 dpi.

To compensate for variations in solar illumination, a calibration target from Mapir was used, as shown in Fig. 2. Figure 2a shows the camera mounted on the UAV, and Figure 2c shows an image of the calibration target in the RGN spectrum Atanasov and Atanasov (2025).

The camera was equipped with an Advanced V2 GNSS receiver module (Mapir, 2025) for Survey3 to provide high-accuracy geolocation data, operating autonomously from the UAV's own GPS.

DJI Mavic 2 Pro and DJI Phantom 4 Pro+ UAVs (DJI, 2025) were used as platforms to carry the camera. Both drones were operated in "P-mode" (Positioning mode), which limits the flight speed to 10 $m \cdot s^{-1}$. The detailed research methodology is described by Atanasov (2024).

Methods used

This study utilises the Normalised Difference Water Index (NDWI) proposed by Gao (1996) to remotely assess water content in the topsoil. Specifically, the version of the index developed by McFeeters (1996) was used, as it is calculated using the green and near-infrared bands available from the mounted RGN camera. The formula is as follows:

$$NDWI = \frac{(G - NIR)}{(G + NIR)} \tag{1}$$

Here, *G* denotes the reflectance in the green spectrum (550 nm) and *NIR* denotes the reflectance in the near-infrared spectrum (850 nm).

According to McFeeters (1996), index values greater than 0.5 typically correspond to water bodies. This phenomenon occurs because water strongly absorbs light in the *NIR* spectrum, causing very low reflectance beyond the visible range.

To analyse the vegetation stage of agricultural crops, the Normalised Difference Vegetation Index (NDVI) is used. This index characterises vegetation density, developmental stage, and the presence of weeds or pathogens, and is also used for yield prediction (Rouse et al., 1974). It is calculated using the following formula:

$$NDWI = \frac{(NIR - R)}{(NIR + R)} \tag{2}$$

where: *R* – the reflectance in the red spectrum (660 nm),
NIR – the reflectance in the near-infrared spectrum (850 nm)

In this study, NDVI data was used to analyse the vegetation stage and determine the degree of crop canopy closure over the field.

Results and discussion

NDWI study results

The 2019–2020 experiments were conducted on an experimental winter wheat field. Observations took place from 28 November 2019 to 10 June 2020. This period was characterised by a severe drought and unusually high temperatures for the region. This is evident from the temperature and precipitation data for November 2019 to June 2020, as shown in Fig. 3.

The winter months experienced atypically high average air temperatures. As a result, the crops began to dry and senesce prematurely. This premature senescence is also reflected in the NDVI trend (Fig. 4b), which shows atypically

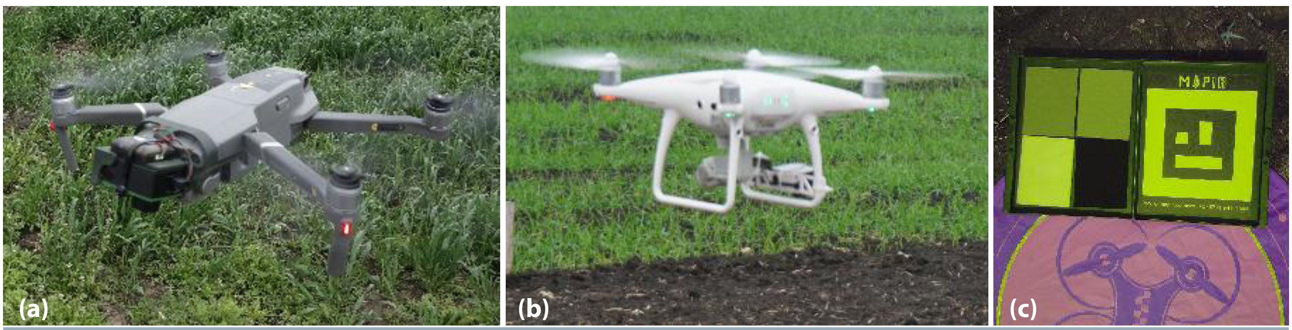

Fig. 2 The equipment used: (a) DJI Mavic 2 Pro; (b) DJI Phantom 4 Pro+; (c) the Mapir calibration target

low values; the index remained negative for almost the entire period. Similarly, the NDWI (Fig. 4a) also remained negative throughout the period, which is consistent with the low precipitation and high air temperatures.

Due to the drought and subsequent wilting of crop leaves, the nadir (90°) view from the UAV primarily captured the soil surface. Consequently, the NDWI values for this period predominantly reflect the moisture content of the topsoil rather than the vegetation.

The climatic conditions for the 2020–2021 season are presented in Fig. 5a. Figure 5b shows the corresponding wind speed data, a factor that directly impacts topsoil moisture.

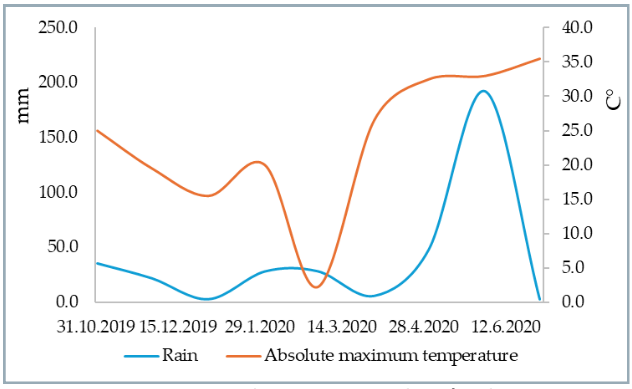

Fig. 3 Temperature and precipitation data for the 2019–2020 period

Figure 6 presents the study of a field with the winter wheat variety Enola (*Triticum aestivum* L.) during the 2020–2021 season. During the winter months, the NDWI values were high, corresponding to significant rainfall (Fig. 5a). A subsequent drought in April and May led to a decrease in the NDWI. Although NDWI values were low in early June, Fig. 6b shows that this coincided with peak NDVI. This indicates a dense vegetation canopy that obscured the soil surface, meaning the NDWI signal at this time primarily reflected the water content within the plants rather than the soil.

Later, as the NDVI decreased in mid-June due to crop ripening and senescence, the soil became more visible. This, combined with renewed rainfall during the same period (Fig. 5a), resulted in an increase in the NDWI values.

Figure 7 presents data on the change in NDWI and NDVI for a field sown with winter sunflower variety SY Onestar CLP near Dobrich. In May, significant precipitation combined with sparse crop cover resulted in high NDWI values, as the signal was dominated by the moisture of the exposed soil. By the end of June, a noticeable drop in NDWI occurred simultaneously with the peak in NDVI. This indicates that the dense sunflower canopy was obscuring the soil, and the NDWI values were therefore reflecting plant water status rather than soil moisture.

High temperatures and low humidity during the summer created drought conditions. As expected, the sunflowers began to ripen and senesce toward the end of August, leading to a decrease in NDVI. As the canopy opened up and

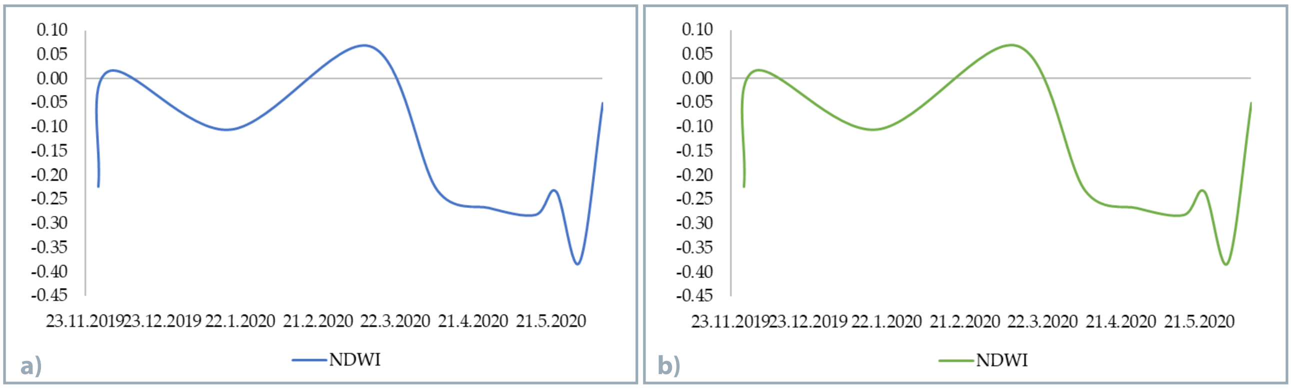

Fig. 4 A comparison of the NDWI (a) and NDVI (b) indices during the 2019–2020 season

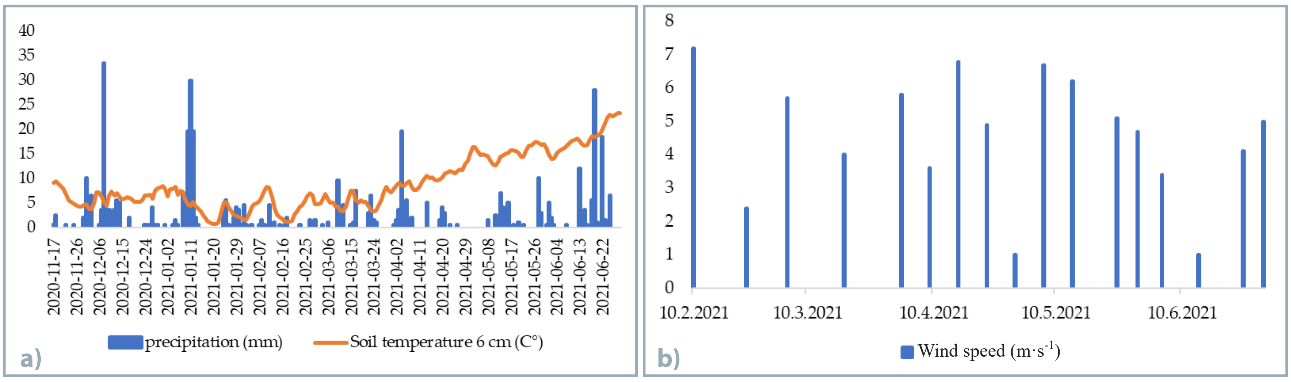

Fig. 5 Atmospheric conditions during the 2020–2021 season: (a) precipitation and air temperature; (b) wind speed measured at the study site

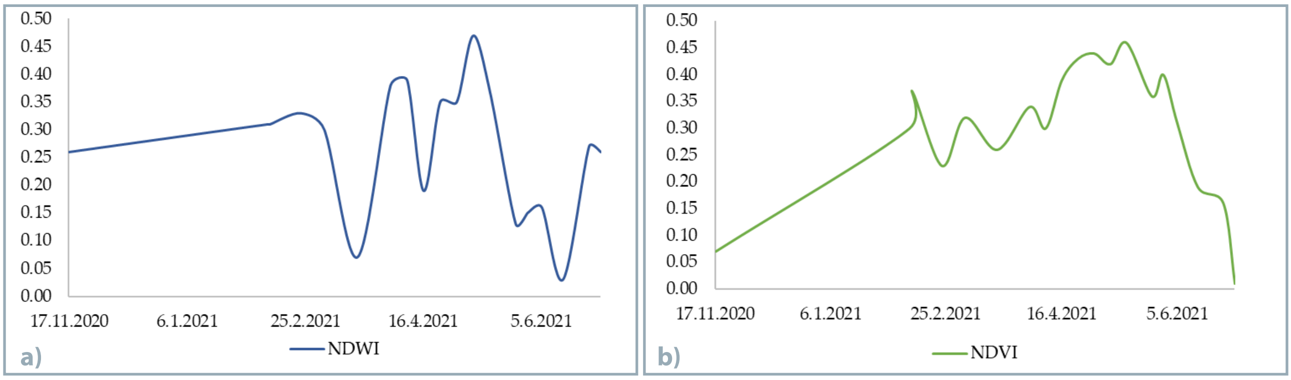

Fig. 6 NDWI (a) and NDVI (b) index values for the winter wheat variety Enola (*Triticum aestivum* L.) in field 3 during the 2020–2021 season

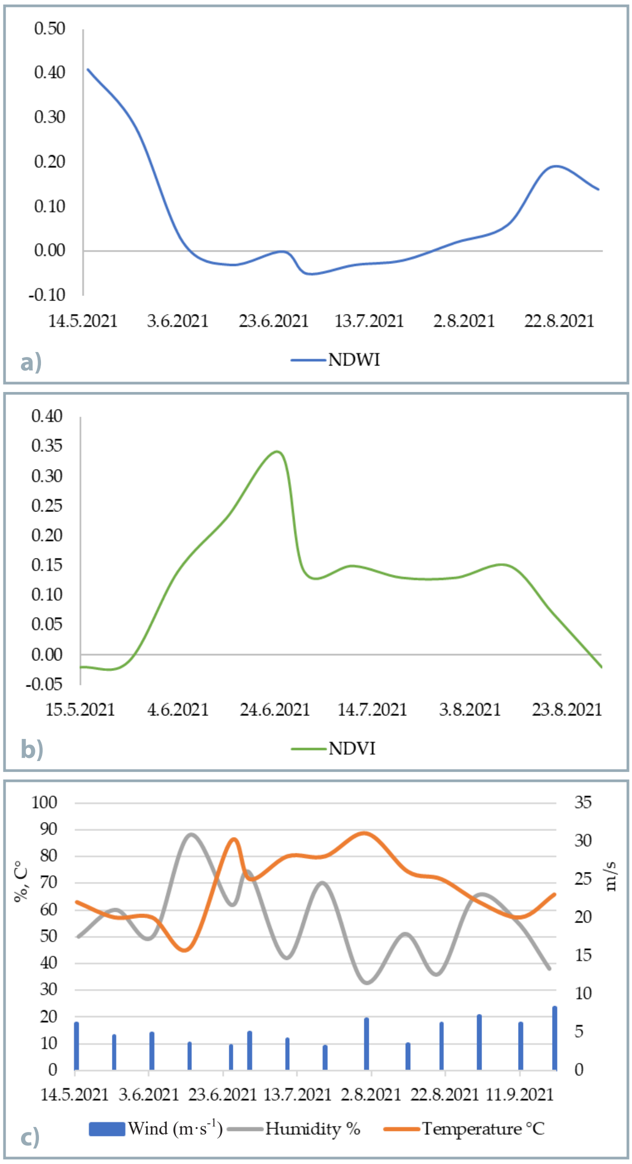

Fig. 7 Index trends for a sunflower field (variety SY Onestar CLP) near Dobrich in 2021, showing (a) NDWI, (b) NDVI, and (c) corresponding atmospheric conditions

following late-summer precipitation, the NDWI values rose again, reflecting the increased visibility of the moist soil.

A maize (*Zea mays*) field during the 2021 growing season is shown in Fig. 8. High NDWI values were observed in May before the crop canopy closed, reflecting the moisture of the exposed soil. As the maize accumulated biomass and NDVI values increased, the dense canopy obscured the ground. Towards the end of the growing season in September, as the crop began to senesce and the canopy opened up, the NDWI signal increased again, reflecting the moisture of the now-visible soil.

The meteorological conditions for the 2021–2022 season are shown in Fig. 9. The figure presents the following data: (a) air temperature dynamics (Fig. 9a), (b) soil temperature

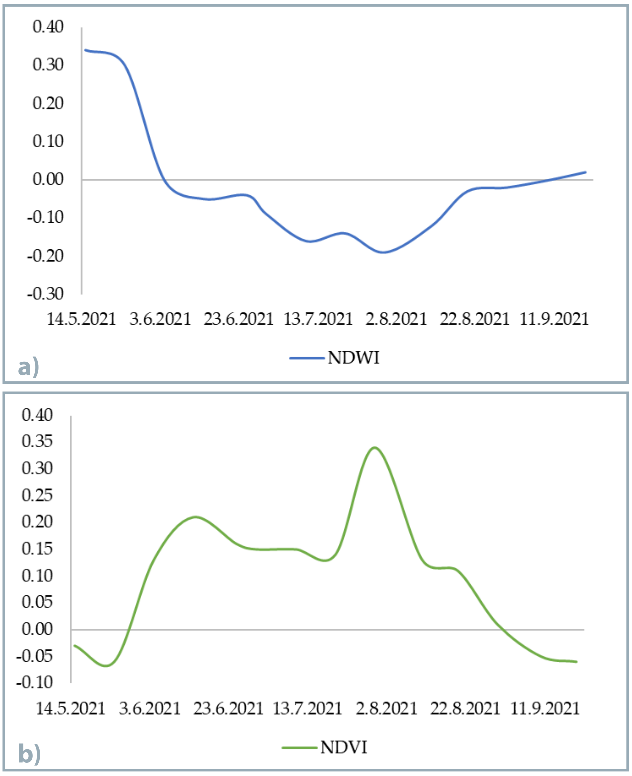

Fig. 8 NDWI (a) and NDVI (b) index trends for a maize (*Zea mays*) field during the 2021 growing season

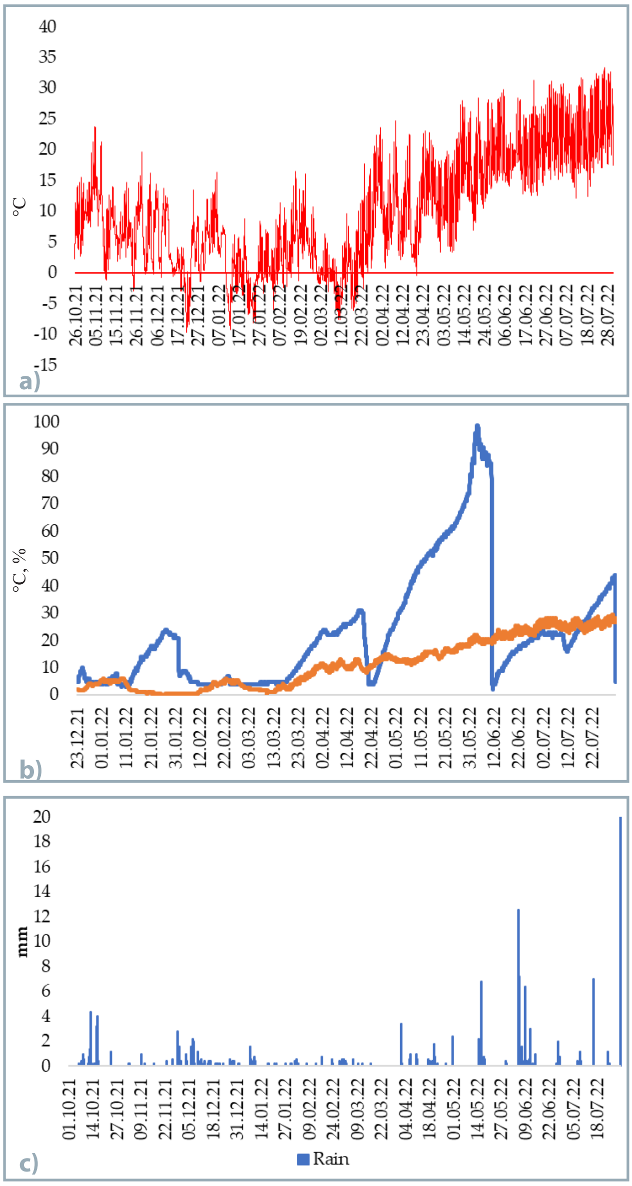

Fig. 9 Meteorological conditions during the 2021–2022 season: (a) air temperature; (b) soil temperature (orange) and soil moisture (blue) at a 6 cm depth; and (c) total precipitation

and soil moisture at a 6 cm depth (Fig. 9b), and (c) total precipitation (9c).

Figure 10 shows the NDWI (a) and NDVI (b) trends for a winter wheat field near General Toshevo during the 2021–2022 season. The data reveals a clear relationship between the indices. In June, as the wheat entered maturity and its NDVI values decreased, the corresponding NDWI values began to rise. This increase in the NDWI coincided with rainfall and directly reflected the higher moisture content in the now-visible soil. Significantly, the trend of the remotely sensed NDWI (the moisture index) strongly correlates with the direct soil moisture measurements presented in Fig. 9b.

Figure 11 presents the NDWI (a) and NDVI (b) trends for a winter wheat field (variety Falado) near Dobrich during the 2021–2022 season. High NDWI values were recorded in November, corresponding to significant precipitation while the crop cover was still sparse. This allowed the index to primarily reflect the moisture of the exposed soil. Conversely, at the end of April, the NDWI dropped noticeably as the NDVI reached its peak. This indicates that the dense crop canopy was obscuring the soil, causing the NDWI to reflect the plant's water status instead of soil moisture.

As expected, following crop ripening and senescence after mid-June, the NDVI decreased. The resulting opening of the canopy, combined with precipitation during this period, led to a subsequent increase in NDWI values as the soil surface became visible again.

The climatic conditions during the 2022–2023 winter wheat season are presented in Fig. 12. The measured soil moisture (Fig. 12b) corresponds to precipitation patterns and decreases as temperatures rise.

The results from the 2022–2023 season show a strong correlation between the indices and the measured environmental conditions. The NDWI values (Fig. 13a) rise in direct correspondence with periods of increased precipitation and higher soil moisture (as shown previously in Fig. 12). Furthermore, the NDVI values (Fig. 13b) also show a positive trend, increasing as soil moisture becomes more available, which promotes healthy vegetation growth.

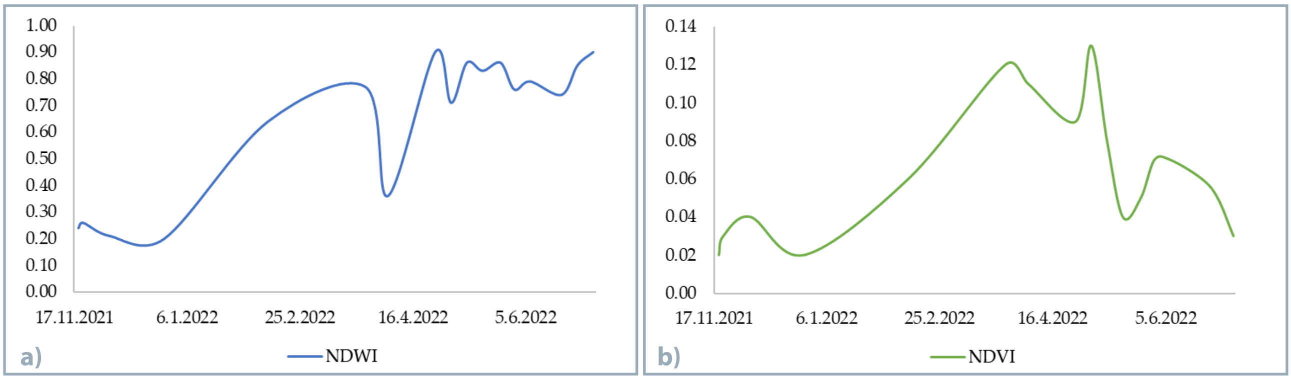

Fig. 10 NDWI (a) and NDVI (b) trends for a winter wheat field near General Toshevo during the 2021–2022 season

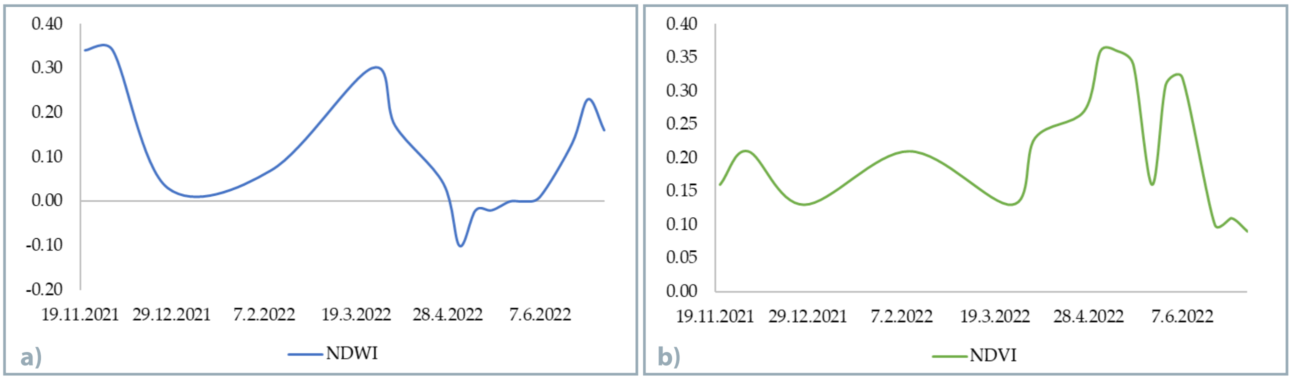

Fig. 11 NDWI (a) and NDVI (b) trends for a winter wheat field (variety Falado) near Dobrich during the 2021–2022 season

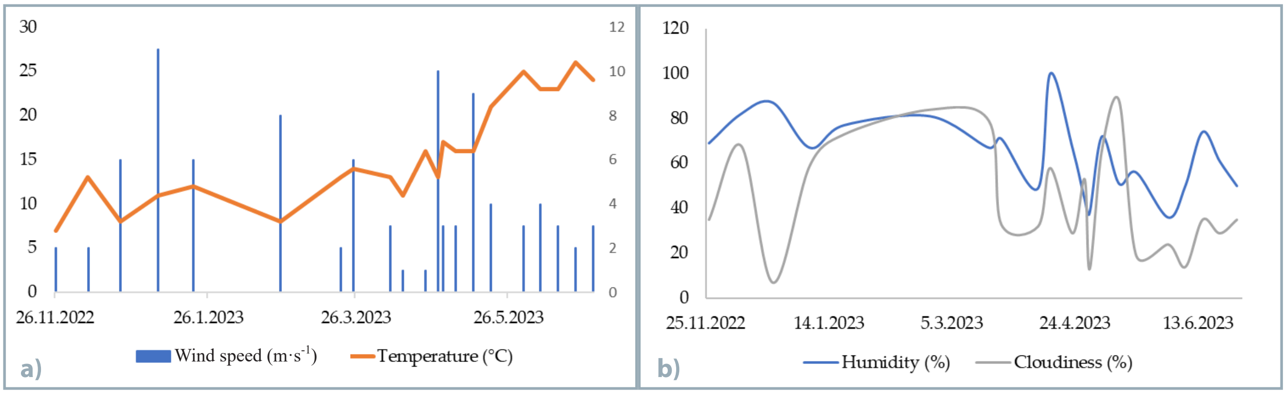

Fig. 12 Atmospheric conditions during the 2022–2023 season: (a) precipitation and air temperature; (b) cloud cover and air humidity

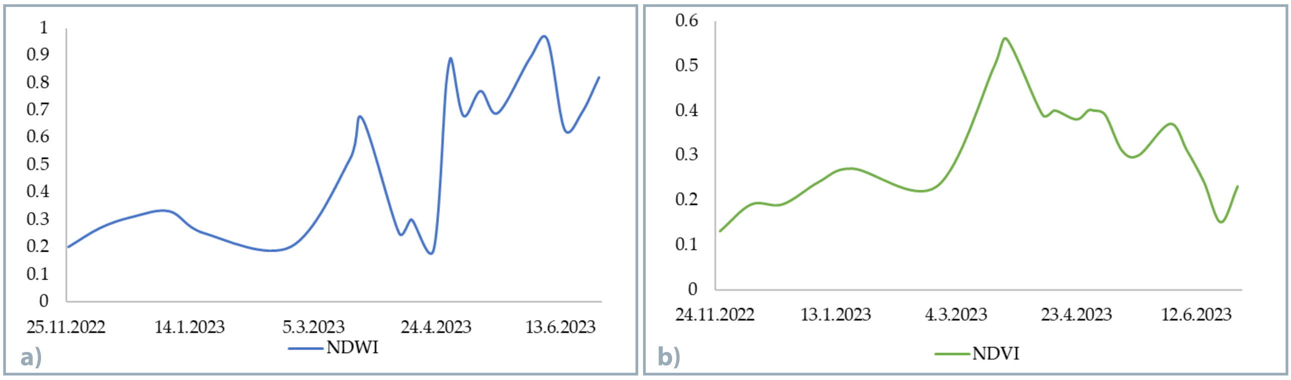

Fig. 13 NDWI (a) and NDVI (b) trends for a winter wheat field near General Toshevo during the 2022–2023 season

Figure 14 shows the change in the moisture index (NDWI) and the corresponding climatic features for a winter wheat field in the Dobrich region during the 2022–2023 season. The data from this period reveals a cyclical interaction between the indices. Following precipitation events, an initial rise in NDWI was observed, reflecting increased soil moisture. This available moisture then promoted vegetation growth, leading to a subsequent increase in NDVI. As the crop canopy became denser (peak NDVI), it obscured the soil, causing the overall NDWI signal to stabilise or decrease as it began reflecting plant water content rather than the saturated soil. At the end of the growing season, rising temperatures and crop maturity led to a decrease in both soil moisture and vegetation health, resulting in a decline in both indices.

The meteorological conditions for the 2023–2024 season are presented in Fig. 15. The data indicates that soil moisture levels changed dynamically in response to precipitation events.

For the corresponding wheat field shown in Fig. 16, the NDWI values increased until mid-February, following a period of rainfall. A decrease in the NDWI was then observed in early March, coinciding with a period of intensive vegetation growth.

In the first ten days of April, a recorded decrease in soil moisture was mirrored by a drop in the remotely sensed NDWI. Finally, at the end of the season, a decrease in NDVI

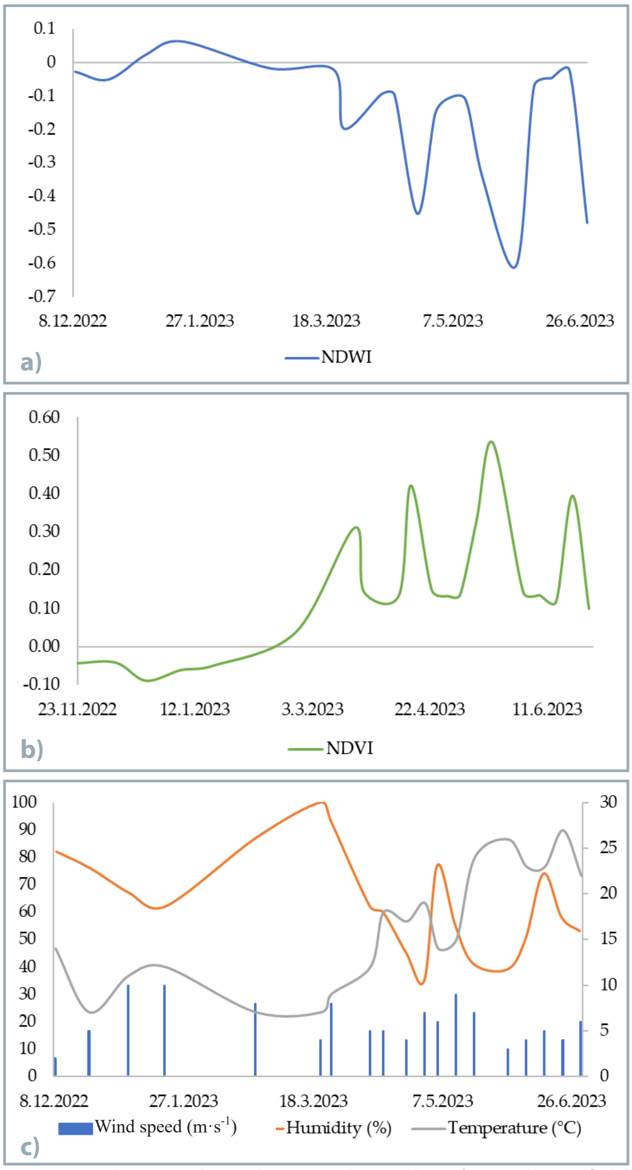

Fig. 14 Index trends and atmospheric data for a wheat field near Dobrich during the 2022–2023 season: (a) NDWI; (b) NDVI; and (c) atmospheric conditions

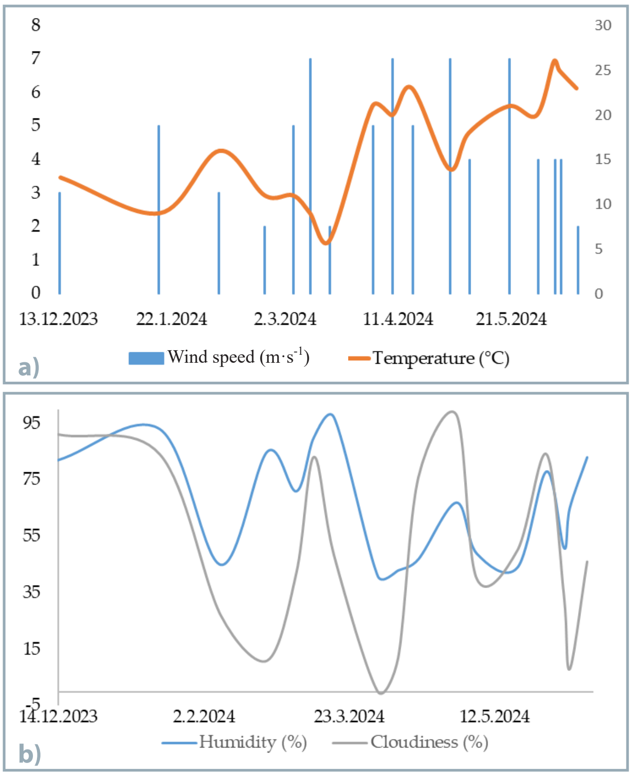

Fig. 15 Atmospheric conditions during the 2023–2024 season: (a) precipitation and air temperature; (b) cloud cover and air humidity

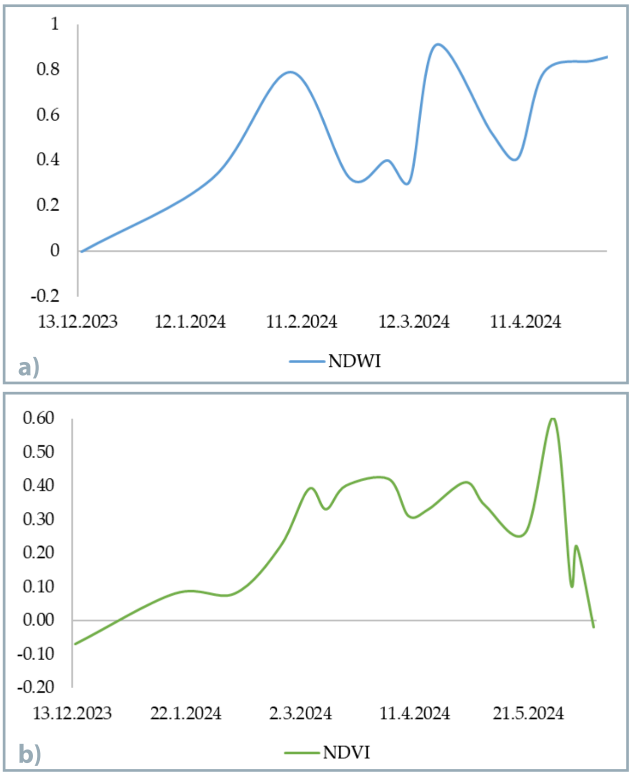

Fig. 16 NDWI (a) and NDVI (b) trends for a field near General Toshevo during the 2023–2024 season

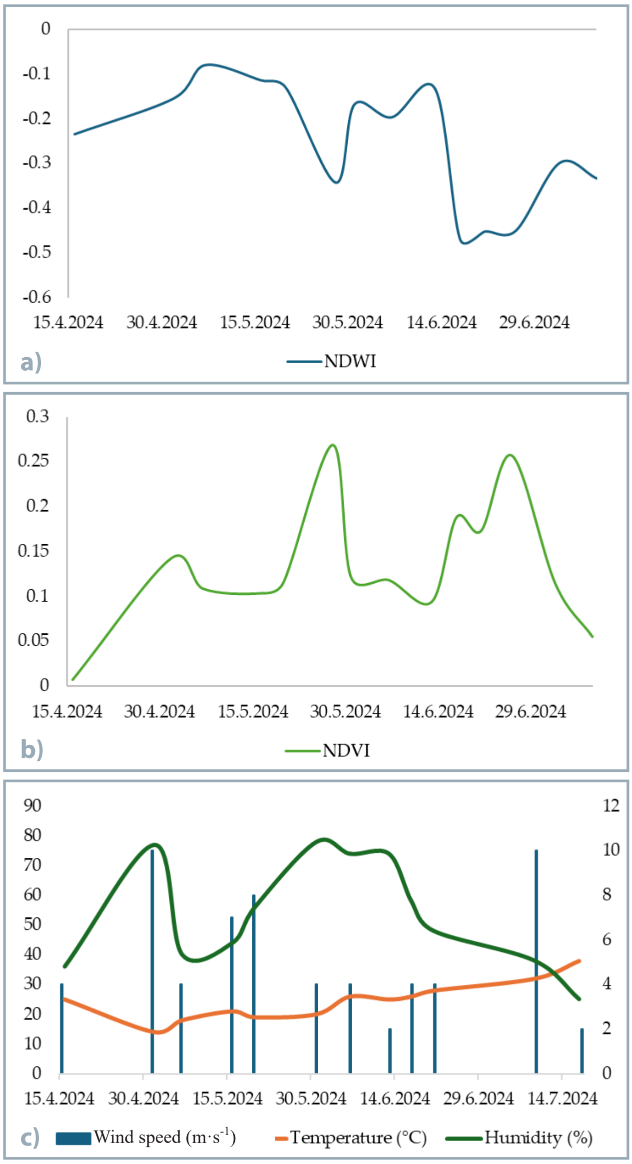

Fig. 17 Index trends and atmospheric data for a triticale field near Dobrich in 2024: (a) NDWI; (b) NDVI; and (c) atmospheric conditions

(due to crop senescence) corresponded with an observed increase in the moisture of the upper soil layer, which was now more visible to the sensor.

Figure 17 presents the index trends and atmospheric data for a triticale field near Dobrich during the 2022–2023 season, showing the NDWI (a), NDVI (b), and corresponding atmospheric conditions (c). The data for April 30th shows that an increase in soil moisture (Fig. 17c) led to a corresponding increase in the NDWI. These favourable conditions subsequently promoted crop development, resulting in an increase in NDVI. By May 30th, while moisture levels remained high, the NDWI value decreased. This coincided with the peak NDVI value, indicating that the dense triticale canopy was obscuring the soil surface. Consequently, the NDWI signal primarily reflected the plant's water status rather than soil moisture. At the end of June, with the onset of crop maturity and senescence, the canopy thinned. This once again allowed for the remote diagnosis of soil moisture, and a corresponding increase in the NDWI was observed. After an increase in the moisture index, an increase in NDVI was also observed.

Zonal map analysis

Figure 18 presents the maps of the topsoil moisture content for a wheat field in November, May, and July. In early November and late July, when the crop canopy was not dense, the index diagnosed the moisture in the upper soil layer. However, as the wheat entered its active development phase, it formed a dense canopy over the soil, and the diagnosed moisture was then primarily within the crop itself.

In May, during the peak vegetation phase, the index registered anomalous zones of both low and high moisture (Fig. 18b). This zoning was unexpected and did not align with previous findings. For comparison, Fig. 19 presents corresponding NDVI maps, used to diagnose the crop's condition on the same dates. In July, the NDVI map (Fig. 19c) shows a general decrease in index values, corresponding with the onset of crop maturity and senescence. Notably, the May NDVI map (Fig. 19b) displays an alternating pattern of low and high index zones, similar to the pattern observed in the NDWI map (Fig. 18b).

A direct comparison revealed an inverse relationship: areas with high NDWI values corresponded to areas with low NDVI values. Ground-truthing confirmed variations in crop density across the field. In zones with low plant density (and thus low NDVI), the larger spacing between plants allowed the sensor to see the moist soil surface, resulting in a high NDWI reading. This field verification validates the accuracy of the remotely sensed data and explains the observed inverse relationship between the two indices.

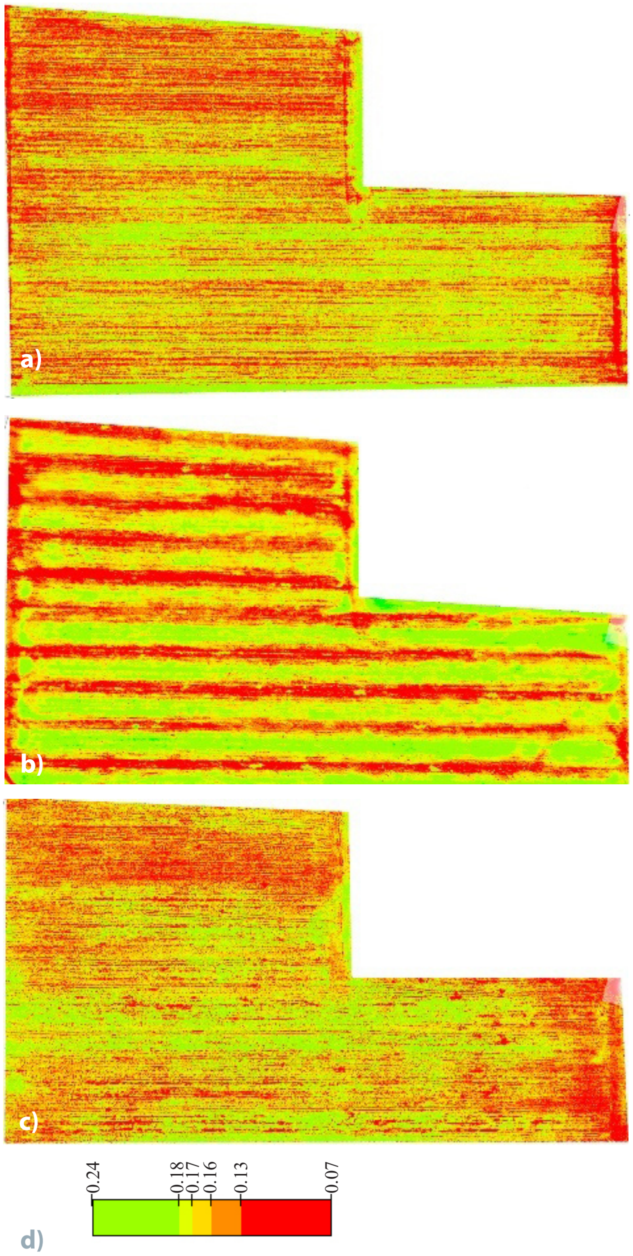

Fig. 18 NDWI index of a wheat field on different dates: (a) 21 November 2022; (b) 25 May 2023; (c) 5 June 2023; (d) colour scale

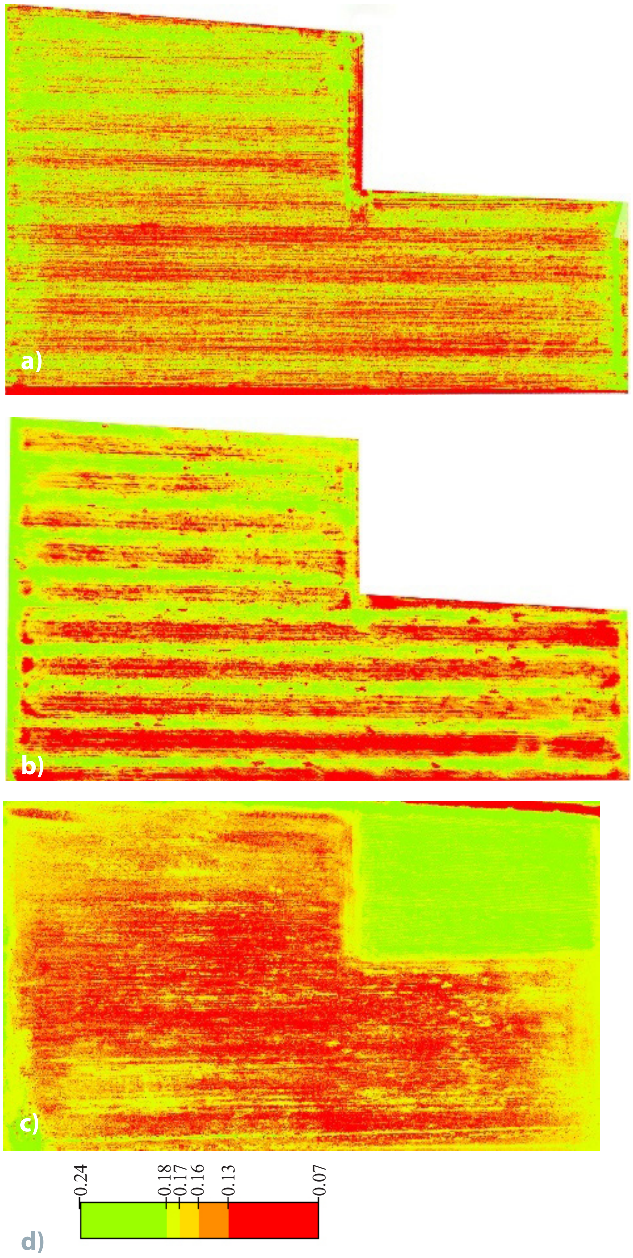

Fig. 19 NDVI index of a wheat field on different dates: (a) 21 November 2022; (b) 25 May 2023; (c) 5 June 2023; (d) colour scale

Data analysis

Data analysis was performed using the Regression function in Microsoft 365 Excel v. 2412 (Microsoft, 2025). For the entire vegetation period, the regression analysis yielded a multiple correlation coefficient (R) of 0.878 and a coefficient of determination (R^2) of 0.771. This indicates that 77.1% of the observed variation in topsoil moisture can be explained by the NDWI values. This suggests a strong correlation between the NDWI and measured topsoil moisture across the entire season. A separate linear regression was performed for the period before crop canopy closure reached 50%. The results for this early-stage analysis were as follows: multiple R: 0.970, R^2: 0.940, adjusted R^2: 1.333, standard error: 0.088, significance F (p-value): 0.025.

The results for this period showed a very strong correlation ($R = 0.970$, $R^2 = 0.940$). This indicates that the NDWI is a highly reliable predictor of topsoil moisture when crop cover is less than 50%. The standard error of 0.088 indicates the average distance that the observed values fall from the regression line. The model was found to be statistically significant, with a p-value (significance F) of 0.025, which is less than the conventional threshold of 0.05. The analysis of residuals showed an average deviation from the predicted regression line of 0.011.

Conclusion

This five-year study, conducted in the Dobruja region using a small UAV to acquire the NDWI, leads to the following conclusions:

- It is possible to effectively monitor topsoil moisture using a small UAV. This method provides a complete spatial overview of the field, unlike traditional point sampling, which only provides discrete values from a few representative locations.
- The NDWI shows a direct relationship with the amount of precipitation and an inverse relationship with soil temperature. The results from the linear regression model are strongest when canopy cover is below 50% ($R^2 \approx 0.94$), and the correlation remains significant even with a dense canopy ($R^2 \approx 0.77$).
- The environmental factors with the most significant influence on the NDWI, in descending order of importance, were found to be: precipitation, relative air humidity, soil temperature, air temperature, and wind speed.

Acknowledgment

The publication of these results was funded by the Technical University of Varna, Bulgaria, under the national programme "Young Scientists and Postdoctoral Fellows – 2".

References

Afshari, S., Sarli, R., Alchin, A.A., Aliabad, O.G., Moradi, F., Saei, M., Lomer, A.R.B., Nasiri, V., 2025. Trend analysis and interactions between surface temperature and vegetation condition: divergent responses across vegetation types. Environmental Monitoring and Assessment 197, 292. https://doi.org/10.1007/s10661-025-13729-9

Alencar Da Silva Allves, K.M., 2024. Application and statistical analysis of multiple water indices based on Landsat 8 reflectance data to detect surface water in a Pampean environment in Argentina. Revista Brasileira de Geografia Fisica 17(2), 1174–1199. https://doi.org/10.26848/rbgf.v17.2.p1174-1199

Alvaro, F., García Del Moral, L.F., Royo, C., 2007. Usefulness of remote sensing for the assessment of growth traits in individual cereal plants grown in the field. International Journal of Remote Sensing 28(11), 2497–2512. https://doi.org/10.1080/01431160600935604

Atanasov, A., 2024. Possibilities of small robotic UAVs for surveillance of agricultural areas in Southern Dobrudzha. Bulgarian Journal of Crop Science 61(3) 100–108. https://doi.org/10.61308/TAGD6115

Atanasov, A., Mihaylov, R., Mihova, G., 2022. Investigating the possibility of monitoring the drying in the upper soil layer by means of a drone in the Dobruja region. In 2022 International Conference Automatics and Informatics (ICAI). Varna, Bulgaria, pp. 115–119. https://doi.org/10.1109/ICAI55857.2022.9960060

Atanasov, A.I., Atanasov, A.Z., 2025. Analysis of opportunities for agricultural area surveillance by UAV and satellite in precision agriculture. Acta Technologica Agriculturae 28(2), 88–96. https://doi.org/10.2478/ata-2025-0012

Chandramohan, K., Elayapillai, P., Vijayalakshmi, G., Kaliraj, S., 2024. Chapter 43 – Evaluating the Relation of NDVI, NDWI, SMI, and LAI to Land and Soil Degradation Processes – a Case Study of Virudhunagar District, Tamil Nadu, India. In: Dharumarajan, S., Kaliraj, S., Adhikari, K., Lalitha, M., Kumar, N. (Eds). Remote Sensing of Soils, Mapping, Monitoring, and Measurement. Elsevier, Amsterdam, The Netherlands, pp. 689–697. ISBN 9780443187735. https://doi.org/10.1016/B978-0-443-18773-5.00040-5

DJI, 2025. Support for Mavic 2. https://www.dji.com/en/mavic-2

Du, J.K., Huang, Y.S., Feng, X.Z, Wang, Z.L., 2001. Study on water bodies extraction and classification from SPOT image. Journal of Remote Sensing 5(3), 214–219.

Gao, B., 1996. NDWI – A normalized difference water index for remote sensing of vegetation liquid water from space. Remote Sensing of Environment 58(3), 257–266. https://doi.org/10.1016/S0034-4257(96)00067-3

Jensen, C.R., Mogensen, V.O., Poulsen, H.H., Henson, I.E., Aagot, S., Hansen, E., Ali, M., Wollenweber, B., 1998. Soil water matric potential rather than water content determines drought responses in field-grown lupin (Lupinus angustifolius). Australian Journal of Plant Physiology 25, 353–363.

Koleva, M., Yankova, P., Plamenov, D., Naskova, P., 2025. Digitalization in plant production and plant protection in Bulgaria – current status and future goals. Annals of the University of Craiova – Agriculture, Montanology, Cadastre Series 54(1), 170–181. https://doi.org/10.52846/aamc.v54i1.1554

MAPIR, 2025. Survey3 Cameras. https://www.mapir.camera/collections/survey3

McFeeters, S.K., 1996. The use of the Normalized Difference Water Index (NDWI) in the delineation of open water features. International Journal of Remote Sensing 17(7), 1425–1432. http://dx.doi.org/10.1080/01431169608948714

Microsoft, 2025. https://www.microsoft.com/en-us/microsoft-365/excel

Pix4D, 2025. Support and Upgrades – PIX4Dfields. https://support.pix4d.com/hc/en-us/articles/360045101131

Rouse, J.W., Haas, R.H., Schell, J.A., Deering, D.W., Harlan, J.C., 1974. Monitoring the Vernal Advancement and Retrogradation (Green Wave Effect) of Natural Vegetation. Type III – Final Report. NASA/GSFC, Greenbelt, Maryland, USA, 390 pp. https://core.ac.uk/download/pdf/42887948.pdf

Toneva, D., Dimitrova, D., 2024. Some aspects of the water crisis in Bulgaria. In Proceedings of the 15th International Scientific and Practical Conference. Vol. 1. Environment. Technology. Resources. Rezekne Academy of Technologies, Rezekne, Latvia, pp. 373–377. https://doi.org/10.17770/etr2024vol1.7972

Ustin, S.L., Roberts, D.A., Pinzón, J., Jacquemoud, S., Gardner, M., Scheer, G., Castañeda, C.M., Palacios-Orueta, A., 1998. Estimating canopy water content of chaparral shrubs using optical methods. Remote Sensing of Environment 65(3), 280–291. https://doi.org/10.1016/S0034-4257(98)00038-8

Wang, L., Qu, J.J., Hao, X., Zhu, Q., 2008. Sensitivity studies of the moisture effects on MODIS SWIR reflectance and vegetation water indices. International Journal of Remote Sensing 29(24), 7065–7075. https://doi.org/10.1080/01431160802226034

Xu, H., 2002. Spatial expansion of urban/town in Fuqing and its driving force analysis. Remote Sensing Technology and Application 17(2), pp. 86–92. https://doi.org/10.11873/j.issn.1004-0323.2002.2.86

Xu, H., 2006. Modification of normalised difference water index (NDWI) to enhance open water features in remotely sensed imagery. International Journal of Remote Sensing 27(14), 3025–3033. https://doi.org/10.1080/01431160600589179